Active Clamp Interleaved Flyback Converter with Single-Capacitor Turn-off Snubber for Stunning Poultry Applications

S. -Y. Tseng, C. -T. Hsieh and H.-C. Lin

GreenPower Evolution Application Research Lab.
(GPEARL)
Department of Electrical Engineering
Chang-Gung University
Kwei-Shan Tao-Yuan , Taiwan, R.O.C
E-mail: sytseng@mail.cgu.edu.tw
TEL: +886-3-2118800
FAX: +886-3-2118026

***Abstract*--The paper proposes an active clamp interleaved flyback converter with a single-capacitor turn-off snubber associated with a full-bridge inverter for stunning poultry applications. The proposed converter can use active clamp circuit to recover the energy of transformer and to achieve zero-voltage switching at turn-on transition. In addition, the proposed one adopts a single-capacitor snubber not only to smooth out switch turn-off transient for reducing turn-off loss but to reduce the ringing voltage of diodes in secondary winding of transformer when switch of the proposed one is operated at turn-on transition. Compared with the counterparts of the conventional converter topologies, the proposed converter has the merits of less component counts, higher efficiency, smaller size, and they are easier to implement. Performance measurements from a prototype have verified feasibility of the overall system design. This designed system has contributed a lot of humane slaughter and has attracted much attention.**

Keywords: **active clamp interleaved flyback converter, single-capacitor snubber, humane slaughter**

I. INTRODUCTION

In recent years, the issue related to welfare of animals has attracted much attention. In particular, livestock and poultry must be rendered unconscious and insensible to pain before they are exsanguinated with humane slaughter methods. In many countries, carbon dioxide (CO_2) and manual electrical stunning are the two methods always used to stun poultry, such as chicken, before slaughtering [1]-[10]. Since the CO_2 method is subject to many limitations and requires higher cost, the manual electrical stunning method has been used more popular.

Poultry stunning is to cause unconsciousness by generating an epileptiform seizure, which includes two phases: a tonic phase and a clonic phase [1]. Degrees of an epileptiform seizure are dependent upon the amount of current passing the brain. The minimum current and voltage required for stunning a chicken is about 40 mA and 60 V, respectively, and they must sustain at least 3s. Conventionally, to generate the specified electrical waveforms, rectified line voltage or battery voltage is chopped into square waveforms with power switches and they are boosted through a low-frequency step-up transformer. As mentioned above, the stunner system is in large volume, size and heavy weight, and there exist bone fractures and ecchymosis in the carcasses of chicken, resulting in low meat quality. To solve above problems, a DC/DC converter with PWM control is adopted for manual electrical stunning applications, which can properly limit current level, regulate output voltage and reduce chicken stress during stunning time.

Since the poultry stunner system belongs to low power level applications, a DC/DC converter with flyback circuit is usually adopted due to its simple circuit structure [11]. To recover energy trapped in leakage inductance of transformer in the flyback converter and achieve zero-voltage switching (ZVS) features at turn-on transition, an active clamp flyback converter is used. Although active clamp flyback can supply an enough power to single-channel poultry stunner system, it doesn't supply an enough power to multi-channel one to speed up poultry slaughter . To relieve this problem, an active clamp flyback with an interleaved manner is adopted, as shown in Fig. 1. Since the active clamp interleaved flyback converter can only solve turn-on switching loss, a single-capacitor turn-off snubber can be used to reduce turn-off switching loss [12], as shown in Fig. 2. Furthermore, when switch M_1 or M_3 is turned on, snubber capacitor C_S and diode D_1 or D_2 form a snubber to avoid the spike voltage across switch M_1 or M_3 due to the resonant network which consists of junction capacitor of diode D_1 or D_2 and leakage inductor of secondary winding in transformer T_{r1} or $T_{r2.}$ As mentioned above, the proposed converter can recover the energy trapped in leakage inductor, achieve zero-voltage switching in switches, and reduce turn–off switching losses significantly.

II. MECHANISM OF POULTRY STUNNING

Carcass quality is highly dependent on the parameters of electrical stunning. For determining the desired

electrical parameters, mechanism of poultry stunning is briefly described. When an enough stunning voltage is applied to the skin of poultry, it will cause an epileptic seizure in the poultry, resulting in a loss consciousness and sensibility. In poultry stunning, degrees of an epileptic seizure are dependent upon the amount of current passing the brain. To generate enough stunning current, a voltage source applied to poultry skin must overcome its impedance.

Electrical properties of skin have been studied over a century and often characterized with impedance spectra a [13], as shown in Fig. 3. An equivalent circuit composed of resistor R_S series with the parallel combination of resistor R_{SC} and capacitor C_{SC} have been used by many investigators to represent the electrical properties of skin, as shown in Fig. 4. Both skin capacitance and resistance have been shown to be proportional to contact area [14]. The skin impedance versus voltage is shown in Fig. 5, illustrating that the skin impedance is reversley proportional to the applied voltage [15].

In general, there are three main parts to form neurons: soma, axon and dendrite. A stimulation signal is sensed by sensory receptors which exist in dermis or subcutaneous layer. When sensory receptors receive into nerve impulse. Its propagation direction is, in turn, through one neuron to the other neurons, in which they are connected in series by synapses, until the nerve impulse propagation is transmitted to a receiver of brain. That is, synapses can play a transducer role which is to transfer electrical stimulation signals to chemical signals, and vice versa, as illustrated in Fig. 6.

To explain the relationship between electrical stunning for poultry and a suppression of nerve impulse propagation, an equivalent circuit for describing the impulse signal propagation between neurons is shown in Fig. 7. In Fig. 7, since synapses play a role of transducer, it can be considered as a switch Q_1. When a voltage E_i is applied then a current I_1 will pass the body of the poultry. In this stunning duration, if current I_1 is large enough, it will induce a high potential V_1 to turn on switch Q_1. When switch Q_1 is turned on, nerve impulse can reach the sensory receivers of the brain through propagation impedance R_i of neuron. As a result, poultry can sense a stimulation signal. As described previously, it can be observed that electrical stunning can inhibit nerve impulse propagation.

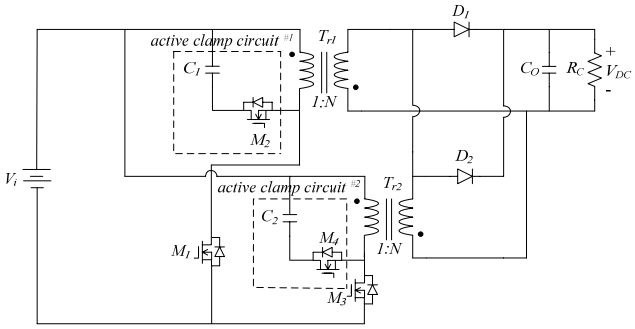

Fig. 1. Schematic diagram of an active clamp flyback converter

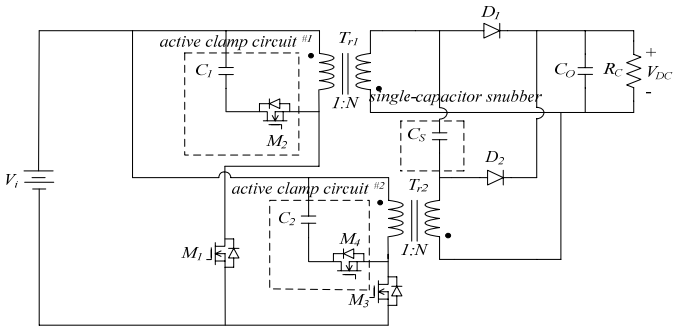

Fig. 2. Schematic diagram of an active clamp flyback converter with a single-capacitor snubber.

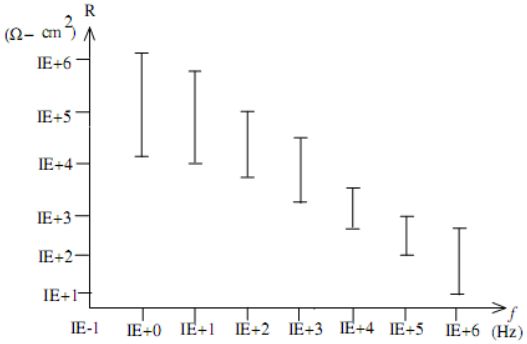

Fig. 3. Illustration of the ranges of skin impedance versus frequency .

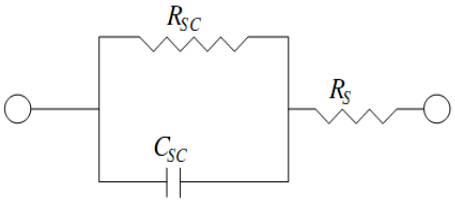

Fig. 4. An equivalent impedance of skin.

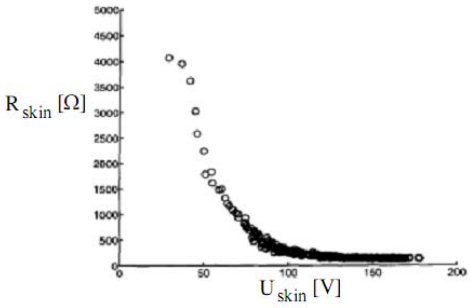

Fig. 5. Plot of the skin impedance of poultry versus the applied voltage.

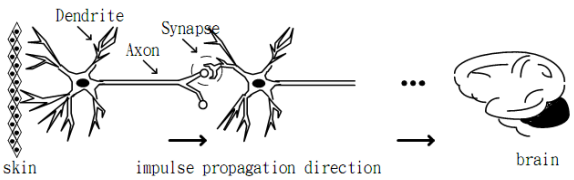

Fig.6. Illustration of impulse propagation between neurons.

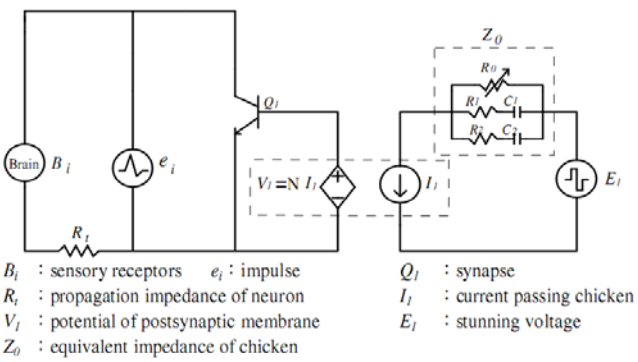

Fig. 7. An equivalent circuit for describing the impulse signal propagation between neurons.

III. OPERATIONAL PRINCIPLE OF THE PROPOSED CONVERTER

The proposed poultry stunning system, an interleaved flyback converter associated with a full-bridge inverter are proposed, as shown in Fig. 8. The interleaved flyback converter can generate a *DC* voltage to supply the full-bridge inverter and use an active clamp circuit and a single-capacitor turn-off snubber to reduce switching losses at turn-on and turn-off transitions. While, the full-bridge one can chop a *DC* voltage into a low frequency square waveform, in which its frequency varies from tens of Hz to hundreds of Hz. In the following, operational principle of the proposed one is briefly described.

Operation of the overall converter is divided into 14 modes. Its each operational mode is shown in Fig. 9 within half one switching cycle. While, their key waveforms are illustrated in Fig. 10. Since operation modes between $t_0 \sim t_7$ are similar to those between $t_7 \sim t_{14}$ except that the operation of switch changes from (M_1 and M_2) to (M_3 and M_4). Thus, each operational mode during half one switching cycle is briefly described as follows.

Mode 1 [Fig. 9(a); $t_0 \le t < t_1$]: Before t_0, diodes D_{11} and D_{21} are in freewheeling, while diode D_{M1} is in forwardly bias. Additionally, leakage inductor L_{K21} and capacitor C_2 are in the resonant manner through switch M_4. Voltage V_{CS} across snubber capacitor C_S is equal to 0. When $t = t_0$, switch M_1 is turned on. Since body diode D_{M1} is in forwardly bias, switch M_1 is operated with zero-voltage switching (ZVS) at turn on. During this time interval, current I_{N22} is the sum of snubber current I_{CS} and diode current I_{D11}. When switch M_1 is turned on, snubber capacitor C_S and secondary winding N_{12} form a low impedance path. Thus, current I_{N22} can be abruptly replaced by $-I_{CS}$. Additionally, switch current I_{DS1} increases from a negative value to 0.

Mode 2[Fig. 9(b); $t_1 \le t < t_2$]: At t_1, capacitor current I_{CS} is equal to $-I_{N22}$, and I_{CS} also equals current I_{N12}. Therefore, diodes D_{11} and D_{21} are reversely biased. Within this time interval, snubber capacitor C_S and magnetizing inductor L_{m21} form a resonant network through transformer T_{r2} and they starts to resonate. While, switch current I_{DS1} is the sum of inductor current I_{Lm11} and I_{N11} which is equal to $-NI_{CS}$. Additionally, leakage inductor L_{K21} and capacitor C_2 still stays in the resonant manner. The energy stored in output capacitor C_O is released to load, and the voltage V_{CS} across snubber capacitor C_s varies from *0* to ($NV_i + V_{DC}$).

Mode 3 [Fig. 9(c); $t_2 \le t < t_3$]: When $t = t_2$, voltage V_{CS} across snubber capacitor C_S is equal to ($NV_i + V_{DC}$) and is clamped at ($NV_i + V_{DC}$). At the same time, diode D_{21} is forwardly biased. During this time interval, magnetizing inductor L_{m11} is in the storing energy state. While, capacitor C_2 and leakage inductor L_{K21} are still kept in the resonant manner. Therefore, inductor current I_{Lm11} increase linearly, while current I_{Lm21} decreases linearly through transformer T_{r2} to output load.

Mode 4 [Fig. 9(d); $t_3 \le t < t_4$]: At t_3, switch M_1 is turned off. At the same time, inductor current I_{Lm11} is sustained in continuous through transformer T_{r1}, snubber capacitor C_s and diode D_{21}. Within this time interval, since the energies trapped in magnetizing inductor L_{m11} and leakage inductor L_{K11} are released to capacitor C_S, C_{M1} and C_{M2}, the voltage V_{DS1} across switch M_1 is smoothed to reduce spike voltage. Therefore, switch M_1 can be operated with zero-voltage transition (ZVT). Additionally, voltage V_{CS} across sunbber capacitor C_S is released to load and its value from ($NV_i + V_o$) to *0*.

Mode 5 [Fig. 9(e); $t_4 \le t < t_5$]: At t_4, voltage V_{DS1} reaches ($V_i + V_{DC}$/N) and voltage V_{CS} across snubber capacitor C_S is nearly equal to *0*. At the moment, diodes D_{M2} and D_{11} are in forwardly bias. Thus, leakage inductor L_{K11} and capacitor C_1 form a resonant network and they starts to resonate. During this time interval, the energies stored in inductors L_{m11} and L_{m21} are released to load through transformers T_{r1} and T_{r2}, and diode D_{11} and D_{21}, respectively .Their currents I_{Lm11} and I_{Lm12} decrease linearly.

Mode 6 [Fig. 9(f); $t_5 \le t < t_6$]: At t_5, switch M_2 is turned on, while switch M_4 is turned off. Since body diode D_{M2} is forwardly biased before switch M_2 is turned on, switch M_2 is operated with ZVS at turn on. During this time interval, leakage inductor L_{K11} and capacitor C_1 are still kept in the resonant manner. Additionally, the energy trapped in leakage inductor L_{K21} is transferred to capacitors C_{M2} and C_{M4}. While, diodes D_{11} and D_{21} are in freewheeling through inductors L_{m11} and L_{m21}, respectively.

Mode 7 [Fig. 9(g); $t_6 \le t < t_7$]: At t_6, voltage V_{DS2} is clamped to *0*, while voltage V_{DS4} is equal to (V_{C2} + V_{DC}/N). During this time interval, diodes D_{11} and D_{21} still stays in freewheeling. Current I_{LK11} abruptly increases from a negative value to *0*. When switch M_3 is turned on at end of mode 7, the other half one switching cycle will start.

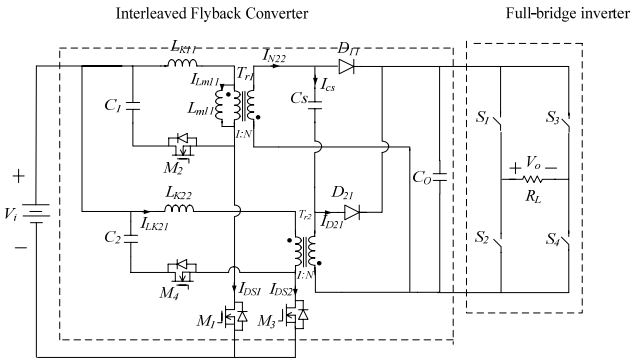

Fig. 8. Schematic diagram of a complete stunners system for stunning poultry applications.

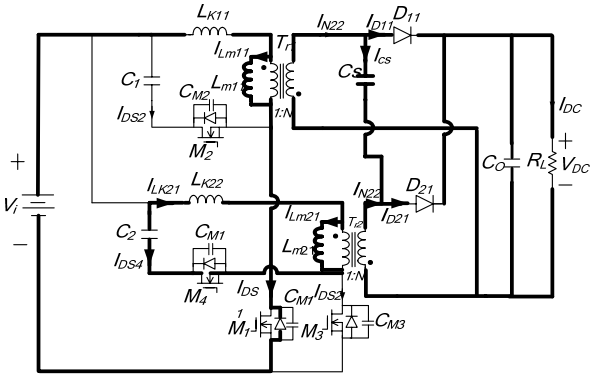

Mode 1 ($t_0 \le t < t_1$)
(a)

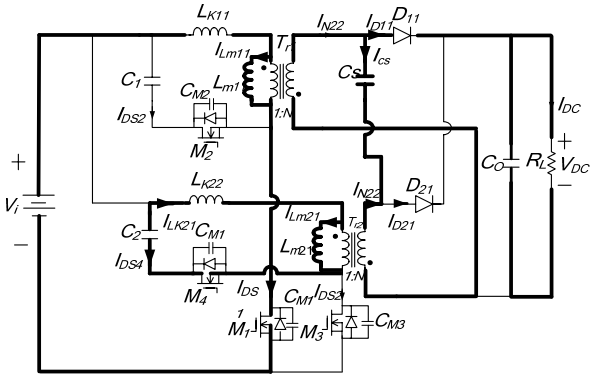

Mode 2 ($t_1 \le t < t_2$)
(b)

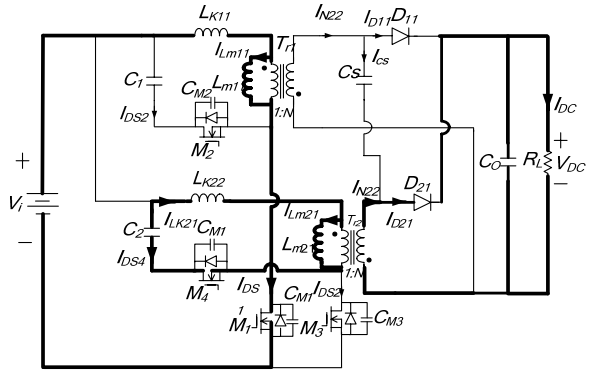

Mode 3 ($t_2 \le t < t_3$)
(c)

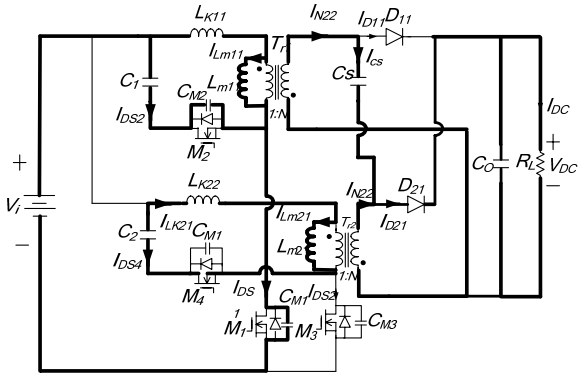

Mode 4 ($t_3 \le t < t_4$)
(d)

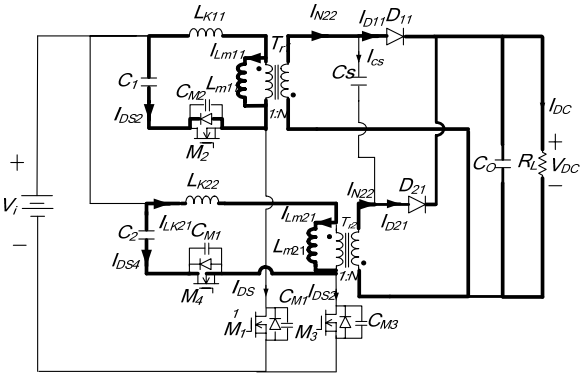

Mode 5 ($t_4 \le t < t_5$)
(e)

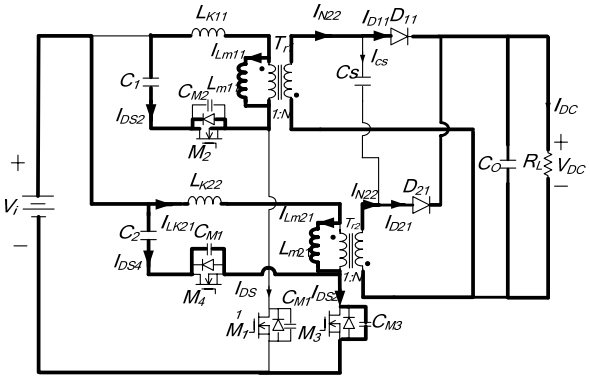

Mode 6 ($t_5 \le t < t_6$)
(f)

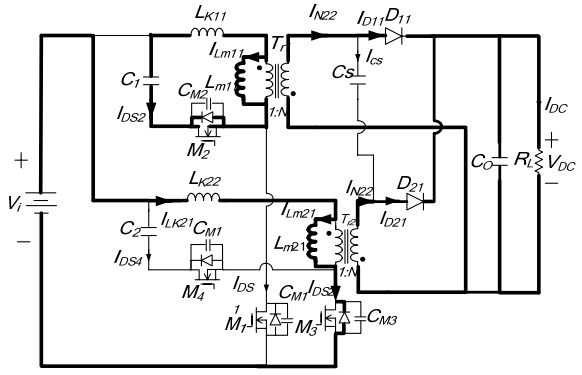

Mode 7 ($t_6 \le t < t_7$)
(g)

Fig. 9. Operational modes of the proposed converter during half one switch cycle.

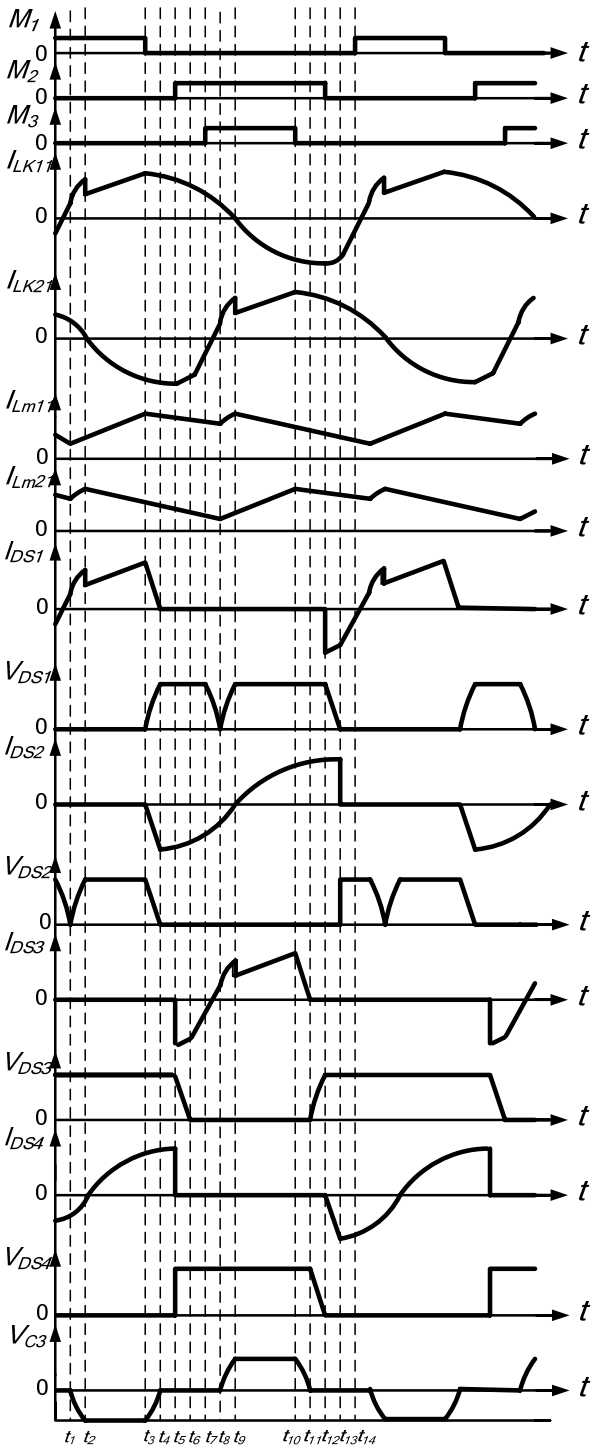

Fig. 10. key waveforms of the proposed active clamp flyback converter with single-capacitor sunbber over one switching cycle.

IV. Design of the Proposed Converter

The proposed converter is composed of an active clamp flyback converter and a single-capacitor snubber. To design the proposed converter systematically, determination of duty ratio D, transformer T_r, active clamp capacitor C_1 (or C_2), snubber capacitor C_S and output capacitor C_O are presented.

A. Duty Ratio *D*

To determine duty ratio, it needs to first obtain input to output voltage transfer ratio M. Since the active clamp circuit and a single-capacitor circuit only help switch M_1 or M_2 to achieve soft-switching feature, they do not affect transfer ratio M of the proposed flyback converter. That is, transfer ratio M will be the same as the conventional one. According to volt-second balance principle, the following equation can be obtained:

$$V_i DT_S + \left(-\frac{V_{DC}}{N}\right)(1-D)T_s = 0, \qquad (1)$$

where N is the turns ratio of transformer T_{r1} (or T_{r2}) and V_{DS} is the output dc-link voltage. From (1), it can be found that transfer ratio M can be expressed as

$$M = \frac{V_{DC}}{V_i} = \frac{ND}{1-D}. \qquad (2)$$

According to (2), once transfer ratio M and turns ratio N are specified, duty ratio D can be determined. Additionally, based on the operational condition of the single-capacitor snubber, duty ratio of switch M_1 or M_2 is limited within 0.5, and switches M_1 and M_2 are operated in complementary. To determine a proper duty ratio, the relationship between duty ratio D and component stress in the proposed converter must be considered. According to (2), a larger duty ratio D corresponds to a smaller transformer turns ratio N, which results in a lower current stress imposed on switches M_1 and M_2, as well as lower voltage stress on freewheeling diodes D_{11} and D_{21}. However, in order to accommodate variations of load, line voltage, component value, and a limited and loss duty, it had better select an operating range between $D =$ 0.3 ~ 0.35.

B. Transformer Tr

Once the duty is selected, the turns ratio of transformer T_r can be determined from (2), which yields

$$N = \frac{(1-D)V_{DC}}{DV_i}. \qquad (3)$$

In the interleaved flyback converter, design values of transformer T_{r1} is the same as those of transformer T_{r2}. By applying the Faraday's law, the number N_{11} of turns at the primary winding can be determined as

$$N_{11} = \frac{DV_i T_S}{A_C \Delta B}, \qquad (4)$$

where A_C is the effectively cross-section area of the transformer core and ΔB is the working flux density. According to (3) and (4), N_{12} can be therefore determined. Similarly, primary winding N_{21} and secondary winding N_{22} of transformer T_{r2} are also determined by (3) and (4).

For the flyback converter, magnetizing inductor L_{m11} of transformer T_{r1} is determined by taking into account the current down slope, which corresponds to the off-time of switch M_1, and the inductance must be large enough to maintain continuous mode (CCM) operation. The inductance of L_{m11} must satisfy the following inequality:

$$L_{m11} \geq \frac{V_{DC}(1-D)T_S}{N^2 \Delta I_{D11(\max)}}, \qquad (5)$$

where $\Delta I_{D11(max)}$ is the maximum ripple of the secondary winding current of transformer T_{r1}, and it is equal to $\Delta I_{Lm11(max)}$/N. When the maximum current ripple is specified, the minimum magnetizing inductance can be determined. Similarly, inductor L_{m21} are also determined by (5).

C. Active Clamp Capacitor C_1 and C_2

The active clamp capacitor C_1 (or C_2) is used to achieve soft-switching feature. To achieve a ZVS feature, the energy stored in inductor L_{K11} (or L_{K21}) must satisfy the following inequality:

$$\frac{1}{2}L_{K11}(I_{LK(tv12)}-I_{LK(tv13)})^2 \geq \frac{1}{2}(C_{M1}+C_{M2})V^2_{DS(\max)} \quad (6)$$

where $L_{K11(tv12)}$ is the leakage inductor current at time t_{12}, $I_{LK(tv13)}$ is that at time t_{13}, C_{M1} and C_{M2} are respectively the junction capacitors of switches M_1 and M_2, and $V_{DS(max)}$ is the voltage across switch M_1 and its value is equal to (V_i +V_{DC}/N). Once C_{M11}、C_{M2}、$I_{LK11(tv12)}$ and $I_{LK11(tv13)}$ are specified, leakage inductor L_{K11} can be determined as

$$L_{K11} \geq \frac{(C_{M1}+C_{M2})V^2_{DS1(\max)}}{(I_{LK11(tv12)}-I_{LK21(tv13)})}. \quad (7)$$

To achieve ZVS feature using active clamp circuit, one half of the resonant period formed by L_{K11} and C_1 should be equal to or greater than the maximum off time of switch M_1. Thus, capacitor C_1 must satisfy the following inequality:

$$\pi\sqrt{L_{K11}C_1} \geq t_{off} = (1-D)T_S. \quad (8)$$

From (8), when L_{k11} is specified, the capacitance range of the clamp capacitor C_1 can be determined as

$$C_1 \geq \frac{(1-D)^2 T_S^2}{\pi^2 L_{K11}}. \quad (9)$$

Similarly, inductor L_{K21} and capacitor C_2 are also determined by (7) and (9), respectively.

D. Snubber capacitor C_S

In the proposed converter, capacitor C_S resonates with inductor L_{m11} or L_{m21} to smooth out switch turn-off transition. The energy stored in C_S can be determined as

$$W_{CS} = \frac{1}{2}C_S(NV_i + V_{DC})^2 \quad (10)$$

To completely eliminate the switch turn-off loss, the energy stored in capacitor C_S must be at least equal to the turn-off w_{soff}, which is expressed by

$$W_{soff} = \frac{t_{soff}}{2}(V_i + V_{DC}/N)I_{DP}, \quad (11)$$

where t_{soff} is the turn-off fall time of switch M_1 and I_{DP} is the current passing the switch. Therefore, capacitor C_S can be determined as

$$C_S \geq \frac{t_{soff} I_{DP}}{N(NV_i + V_{DC})} \quad (12)$$

E. Output capacitor C_O

The output capacitor C_O is primarily designed for reducing ripple voltage. The ripple voltage across output capacitor C_O is determined as follows:

$$\Delta V_{rco} = \frac{\Delta Q_{CO}}{C_O} = \frac{1}{C_O}(I_{O(\max)} \times \frac{DT_S}{2}) = \frac{DI_{O(\max)}T_S}{2C_O}, \quad (13)$$

where $I_{O(max)}$ is the maximum output current.

V. Measure Results

To verify the performance of the proposed intelligent stunner, as shown in Fig. 8, a prototype with the following specifications was implemented.

A. Active Clamp Flyback Converter

- input voltage V_i: 150 V_{DC},
- switching frequency f_{S1}: 50 kHz,
- output voltage V_{DC}: 120 V_{DC}, and
- maximum output current I_{DC}: 2 A.

B. Full-Bridge Inverter

- input voltage V_{DC}: 120 V_{DC},
- maximum output power: 240 W,
- output voltage V_O: 120 V,
- maximum output current I_O: 2 A, and
- switching frequency f_{S2}: 400 Hz.

According to the specifications, components of the active clamp flyback converter associated with turn-off snubber are determined as follows:

- turns ratio of transformers T_{r1} and T_{r2}: 1,
- magnetizing inductors $L_{m11}$and L_{m21}: 627 μH
- transformer core: EI-42,
- leakage inductors $L_{K11}$and L_{K21}: 7.32 μH,
- switches M_1 and M_2: IRF840, and
- diodes D_{11} and D_{21}: UF304.

To generate ac voltage waveforms, the switches of the full-bridge inverter are also determined as S_1 ~ S_4: IRF840.

Measure waveforms of V_{DS} and I_{DS} of switches M_1 and M_3 are shown in Figs. 11 (a) and (b) at 50% of the full load, from which it can be seen that the proposed converter can achieve ZVS features at turn-on transition and ZVT at turn-off transition. Figs. 12 (a) and (b) show measured waveforms of V_{DS} of switches M_2 and M_4, illustrating that switches M_1 and M_2 can be operated with ZVS at turn-on transition. Efficiency comparison between the proposed converter and conventional interleaved one with hard-switching circuit is depicted in Fig. 13. From Fig. 13, it can be seen that the proposed converter can yield higher efficiency over the conventional one, and its efficiency is 92% under full load condition. In addition, the efficiency of the overall stunner system is 85% under full load condition. Fig.14 shows measured waveforms of DC-link voltage V_{DC} and

output voltage V_O of the stunner system under a load of ±2 A, in which the waveforms are with frequency of 400 Hz and ratio of 50%. From Fig. 14, it can be observed that the output voltage has been regulate within 1%, improving meat quality significantly. Measured waveforms of output voltage V_O and output current I_O during goose stunning interval are shown in Fig. 15, from which it can be found that the poultry stunner with the proposed stunner system is first controlled with the regulation voltage manner. Then, when output current I_O is greater that a set value of 350 mA, the proposed one will enter the regulation current manner to sustain constant output current. Form Fig. 15, it can be seen that the poultry stunner with the proposed stunner system can reduce poultry stress and increase meat quality. Additionally, from practical experimental results for stunning a goose, it can be observed that the coma time of goose under voltage of 120 V, current of 350 mA, and stunning time of 6s can sustain about 30s, and it is long enough for bleeding.

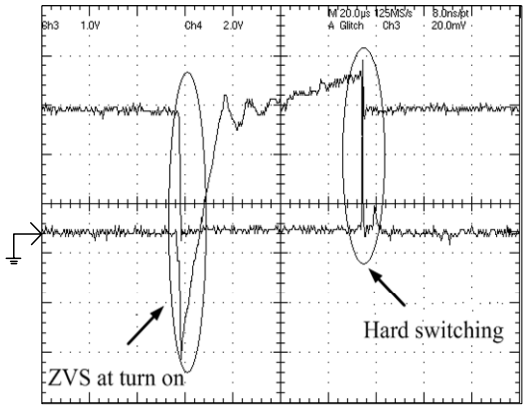

(100 V/div , 0.5 A/div , 2 μs/div)
(a)

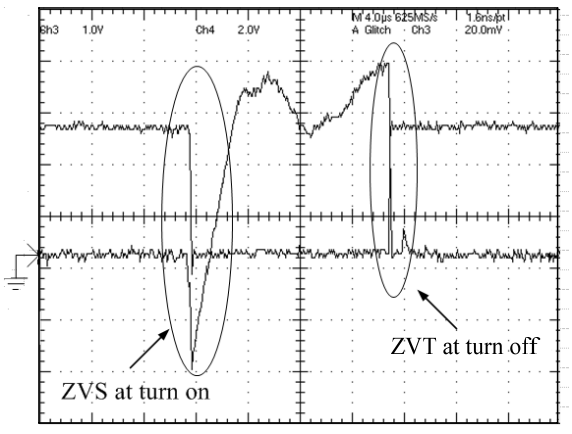

(100 V/div , 0.5 A/div , 2 μs/div)
(b)

Fig. 11. Measured voltage V_{DS} and current I_{DS} waveforms of (a) switch M_1, and (b) switch M_3 in the active clamp converter with the single-capacitor snubber, illustrating ZVS at turn on and ZVT at turn off under 50% of the full load.

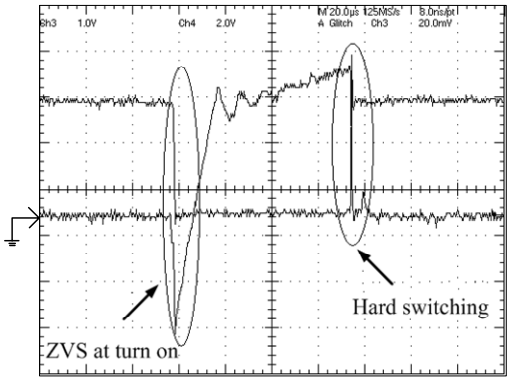

(100 V/div , 0.5 A/div , 2 μs/div)
(a)

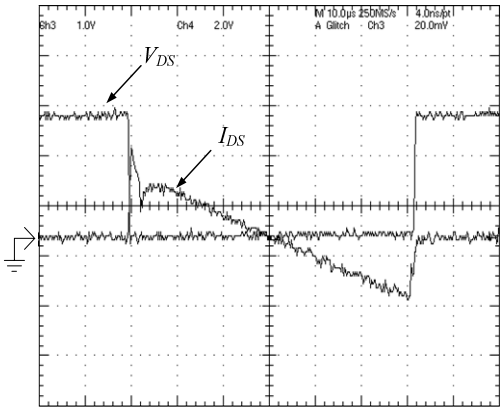

(100 V/div , 0.5 A/div , 2 μs/div)
(b)

Fig. 12. Measured voltage V_{DS} and current I_{DS} waveforms of (a) switch M_2, and (b) switch M_4 under 50% of full load in the proposed converter, illustrating ZVS at turn on.

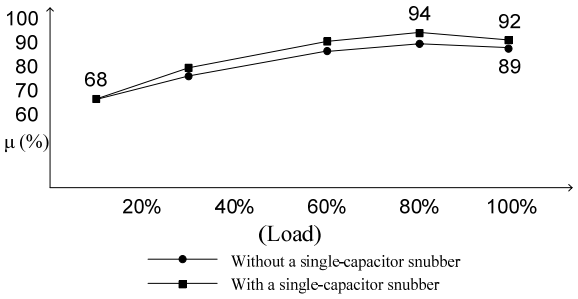

Fig. 13. Comparison conversion efficiency between the active clamp interleaved flyback converter without a single-capacitor snubber and the proposed one.

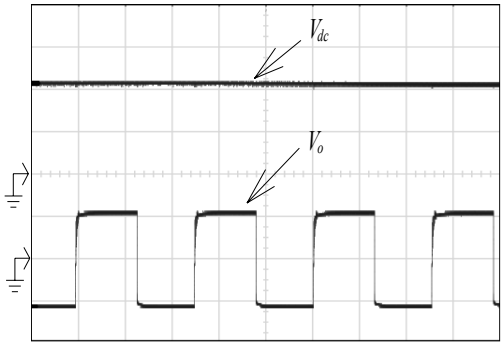

(V_{DC} : 50 V/div, V_o : 100 V/div, 1 ms/div)

Fig. 14. Measured waveforms of dc output voltage V_{DC} and output voltage V_o under a load of ±2 A.

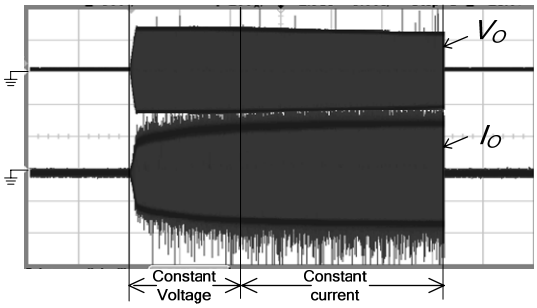

(V_O : 100 V/div, I_o : 200 mA/div, 1 s/div)

Fig. 15. Measured waveforms of output voltage V_o and output current I_o during chicken stunning interval.

VI. Conclusion

In this paper, coma mechanism of poultry with electrical stunning has been briefly reviewed. Operational principle, steady-state analysis and design of the proposed active clamp converter with a single-capacitor snubber associated with full-bridge inverter has been implemented to generate stunning electrical parameters, in which its current amplitude is 350 mA and its voltage amplitude is 120 V. In addition, the proposed interleaved active-clamp flyback converter with the single-capacitor snubber can achieve the efficiency around 92 % under full load condition, and the efficiency of overall stunner system is about is about 85 %. From experimental results, it can also found that proposed one can attain a good meat quality, which meet the regulation of animal welfare.

Reference

[1] H. A. Channon, A. M. Payne and R. D. Warner, "Comparison of CO2 Stunninng with Manual Electrical Stunning (50Hz) of Pig on Carcass and Meat Quality," *Trans. on Meat Science*, 2002, pp.63–68.

[2] S. B. Wotton and M. O. Callaghan, "Electrical Stunning of Pigs: the Effect of Applied Voltage on Impedance to Current Flow and the Operation of a Fail-Safe Device," *Trans. on Meat Science*, 2002, pp. 203–208.

[3] A. Velarde, *et al.*, "Effect of Electrical Stunning on Meat and Carcass Quality in Lambs," *Trans. on Meat Science*, 2003, pp. 35–38.

[4] H. A. Channon, A. M. Payne and R. D. Warner, "Effect of Stun Duration and Current Level Applied During Head to Back and Head only Electrical Stunning of Pigs on Pork Quality Compared with Pigs Stunned with CO2, " *Trans. on Meat Science*, 2001, pp. 1325–1333.

[5] E. Lambooij, *et al*., "Some neural and behavioural aspects of electrical and mechanical stunning in ostriches," *Trans. on Meat Science*, 1999, pp. 339–345.

[6] E. Lambooij, *et al* l., "The Effects of Captive Bolt and Electrical Stunnin, and Restraining Methods on Broiler Meat Quality," *Trans. on Poultry Scien ce*, 1999, pp. 600–607.

[7] B. Savenije, *et al*., "Electrical Stunning and Exsanguination Decrease the Extracellular Volume in the Broiler Brain as Studied with Brain Impedance Recordings," *Trans. on Poultry Science*, 2000, pp. 1062–1066.

[8] V. Sante, *et al*., "Effect of Stunning Current Frequency on Carcass Downgrading and Meat Quality of Turkey," *Trans. on Poultry Science*, 2000, pp. 1208–1214.

[9] S.F. Bilgili, "Recent Advances in Electrical Stunning," *Trans. on Poultry Science*, 1999, pp. 282–286.

[10] W. D. McNeal, *et al*., "Effects of Stunning and Decapitation on Broiler Activity During Bleeding, Blood Loss, Carcass, and Breast Meat Quality," *Trans. on Poultry Science*, 2003, pp. 163–168.

[11] R. Watson, F. C. Lee and G. C. Hua, "Utilization of an Active-clamp Circuit to Achieve Soft Switching in Flyback Converters," *IEEE Trans. on Power Electronics*, Vol. 11, Jan. 1996, pp.162 – 169.

[12] J. Du and H. Ohsaki, "Numerical analysis of eddy current in the EMS-maglev system." Proc. of 6th Int. Conf. on Electrical Machines and Systems (ICEMS 2003), Beijing (China), Nov. 2003, pp.761-764.

[13] M. R. Prausnitz, "The Effects of Electric Current Applied to Skin: A Review for Transdermal Drug Delivery," Proceedings of the Advanced Drug Delivery Reviews, Vol. 18, 1996, pp. 395-425.

[14] U. Pliquett, R. Langer and J. C. Weaver, "Changes in the Passive Electrical Properties of Human Stratum Corneum Due to Electroporation,"Trans. On Biophysica Acta, 1995, pp.111–121.

[15] M. R. Prausnitz, "A Practical Assessment of Transdermal Drug Delivery by Skin Electroporation," Proceedings of the Advanced Drug Delivery Reviews, Vol. 35, 1999, pp. 61–7.